

# On the prediction of the design criteria for modification of contact stresses due to thermal stresses in the gear mesh

Ebubekir Atan\*

*Department of Mechanical Engineering, Izmir Institute of Technology, Urla, Izmir 35430, Turkey*

## Abstract

The mechanism of surface failure due to temperature rise is a very important problem in gear design. Thermal considerations have received considerable attention from the gear researchers but only for scoring failures when the destruction of lubrication film occurs as a result of temperature rise. In spite of the wealth of literature on this subject, this problem is not fully analyzed.

The objectives of this paper are to consider the mechanisms of thermal stresses and the thermal cycling in contact zone, during the gear mesh. This research has been conducted for the first point of contact based on consideration of transient heat transfer, elastohydrodynamic lubrications, and surface roughness and gear material.

A procedure presented in this paper evaluating the stresses (thermal and mechanical) and predicting the design criteria for modifying the contact stresses due to thermal stresses. The effect of the material, oil film thickness, surface roughness and geometric operating parameters on modification parameter is illustrated. Also the effects of a load on the temperature rise and the modification parameters are evaluated.

© 2004 Elsevier Ltd. All rights reserved.

*Keywords:* Transient temperature rise; Thermal stress effect; Gear tooth surface failure

## 1. Introduction

Although most of the failures of gears are surface failures, the interaction among the factors influencing these failures is not yet fully understood. The most common types of surface failures are usually classified as pitting, wear and scoring.

In the past, there was a tendency to regard micro pitting as a secondary wear problem and most of the attention focused on macroscopic pitting, which is attributed to contact fatigue. It is seen in rolling element bearing and gears when the Hertzian pressure exceeds an allowable value. The crack usually propagates for a short distance in a direction roughly parallel to the tooth surface before turning up or branching to the surface. Webster and Norbart [1] investigated the effect of various parameters on a type of progressive fatigue wear known as micro pitting. They concluded that increasing the load, decreasing specific film

thickness and maintaining negative relative sliding all increased the rate of micro-pitting wear. They also reported that micro pitting is almost completely eliminated at very low, but non-zero, slide to roll ratio.

Tallian [2] investigated the role of surface defects in spalling life prediction modelling. His efforts concentrated on micro spalling, in asperity dimensions. He analyzed surface distress defect formation in rolling contact using the Greenwood–Williamson surface roughness model. He suggests a significant influence on life of several parameters, such as EHL film thickness ratio, traction, material fatigue properties, and pre-service defects.

Lin, Cheng, and Jang [3] conducted experiments to measure the wear behaviour of simulated lubricated gear contacts. They reported that the effect of applied load on wear is more significant than the effect of speed. They also reported that the oil temperatures increased as the sliding speed or the applied loads are increased. Kopf [4] investigated the phenomenon that progressive wear at some critical point caused a rapid increase in wear rate, distortion of the tooth profiles and the failure of the gear transmission.

\* Tel.: +90 232 750 6634; fax: +90 232 750 6505.

E-mail address: ebubekiratan@iyte.edu.tr

## Nomenclature

$\lambda$	is lubrication parameter	$\alpha_t$	thermal expansion coefficient ( $\mu\text{m}/\text{m}^\circ\text{C}$ )
$h$	is lubrication film thickness (m)	$\nu_1, \nu_2$	poisson's ratio of pinion and gear materials, respectively
$\sigma_{\text{rms}}$	is asperities root-mean square height (m)	$\sigma_m$	the mechanical tensile stress on the surface (Pa)
$q$	transient heat flux (W)	$\sigma_t$	the thermal tensile stress on the surface (Pa)
$R_{C1}, R_{C2}$	effective radius of curvature of the contacting surfaces (m)	$\sigma_u$	the ultimate tensile strength (Pa)
$R_p, R_g$	pitch radii of pinion and gear, respectively, (m)	$(\sigma_m)_{\text{all}}, (\sigma_c)_{\text{all}}$ and $(\sigma_t)_{\text{all}}$	the allowable mechanical, combined and thermal stresses for infinite life, respectively
$R_{b1}, R_{b2}$	base circle radii of pinion and gear, respectively, (m)	$K_m$	the ratio of the fatigue limit due to mechanical loading to the ultimate tensile strength
$R_{01}, R_{02}$	addendum circle radii of pinion and gear, respectively, (m)	$K_t$	the ratio of the thermal fatigue limit to the ultimate tensile strength
$A_c$ and $A_0$	the real and nominal contact areas, respectively, ( $\text{m}^2$ )	$K$	stress modification factor
$R_q$	the constant asperity radius (m)	$x_s$	relative position of the starting point of contact, (along the line of action)
$T_{01}$	the maximum fluid film temperature ( $^\circ\text{C}$ )	$M_g$	gear ratio ( $N_g/N_p$ )
$T_{s1}$	the maximum surface temperature ( $^\circ\text{C}$ )	$\phi$	pressure angle of the gear tooth (degree)
$T_{B1}$	the bulk temperature ( $^\circ\text{C}$ )	$E_1, E_2, E_c$	of modulus of elasticity of pinion, gear and equivalent, respectively, (Pa)
$\psi$	the heat partition of coefficient (assumed 0.5)	$f$	coefficient of friction
$V_1$	speed of radii of curvature of pinion teeth surface at start of contact point (m/s)	$C_d$	centre distance (m)
$V_s$	sliding velocity	$r_1$	pitch radii of pinion (m)
$\rho_1$ and $\rho_0$	the densities of gear material and fluid ( $\text{kg}/\text{m}^3$ )	$b$	hertzian contact width (m)
$c_1$ and $c_0$	the specific heats of material and fluid ( $\text{J}/\text{kg}^\circ\text{C}$ )	$\omega_1$	angular velocity of pinion (rad/s)
$k_1$ and $k_0$	the conductive heat transfer coefficient of material and the fluid ( $\text{W}/\text{m}^\circ\text{C}$ )	$P$	transmitted power (W)
$b$	the contact width (m)		

Terauchi [5] reported on extensive experiments on the failure of the tooth surfaces of spur gears due to scoring. He examined the main factors influencing the scoring resistance of the gears, such as the number of teeth, tooth profile modification, module, and the mechanical and thermal properties of the gear materials and the lubricants. He concluded that, based on the assumption that the danger of scoring could be estimated from the evaluation flash temperature at the meshing faces. An expression for the estimation of scoring resistance of the gears would not be reliable.

## 2. Temperature rise calculation in lubricated rough surface contact

In this paper, the temperature rise on the bulk surface and the asperities are calculated based on whether the rise resulted from frictional heat or viscous heat generation. The considered lubrication conditions are given below.

The bulk surface is always covered with the lubricant. Therefore, the temperature rise is calculated based on viscous heating.

The asperity temperature rises are calculated based on the condition of the lubrication parameter,  $\lambda$  as given

below:

$$\lambda = \frac{h}{\sigma_{\text{rms}}} \quad (1)$$

Temperature rises are calculated based on frictional heating when the lubrication parameter  $\lambda \leq 1.4$  implies some asperity interaction and calculated based on viscous heating when lubrication parameter  $\lambda > 1.4$  implies negligible asperity interaction [6].

### 2.1. Temperature rise calculation based on frictional heating

The frictional temperature rise for the pinion and gear at the start of contact, where the maximum sliding velocity and temperature rise occurs, can be determined by assuming two cylinders with radii corresponding to the radii of curvature of the teeth at the contact point as shown in Fig. 1. The maximum transient temperature rise at the asperities of the pinion ( $\Delta T$ ) calculated as an extension of the analysis given by Taylor and Seireg [7] as expressed below

$$\Delta T = \frac{2q}{\sqrt{\pi k_1 \rho_1 c_1}} \sqrt{t} \quad (2)$$

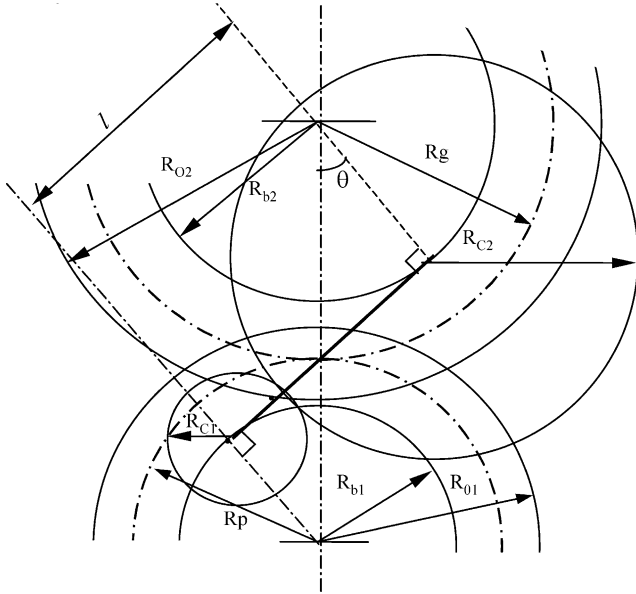


Fig. 1. Equivalent contacting cylinders with radius  $R_{C1}$  and  $R_{C2}$  for tooth profiles of meshing gears.

where

$q$  transient heat flux  
 $t$  time duration for heat flux application.

The Eq. (2) can be applied for the start of contact in the pinion and gear as below in four groups of parameters:

Material parameters  $\phi_1(\nu_1, \nu_2, \rho_1, E_1, E_2, k_1, c_1)$ ,  
 Geometric parameters  $\phi_2(M_g, N_p, \phi, x_s)$ ,  
 Lubrication and surface parameters  $\phi_3(\psi, f, A_0/A_c)$ ,  
 Application parameters  $\phi_4(P, \omega_1, C_d)$ ,

$$\Delta T_p \equiv \phi_1(\nu_1, \nu_2, \rho_1, E_1, E_2, k_1, c_1) \phi_2(M_g, N_p, \phi, x_s) \phi_3(\psi, f, A_0/A_c) \phi_4(P, \omega_1, C_d)$$

$$\Delta T_p = \frac{1}{\pi^{1/4}} \left( \frac{1}{\left( \frac{1-\nu_1^2}{E_1} + \frac{1-\nu_2^2}{E_2} \right)^{1/4} \sqrt{k_1 \rho_1 c_1}} \right) \times \left( \frac{(1 + M_g)^{3/4} [1 - (M_g + 1)x_s] \sin^{1/4} \phi}{M_g x_s^{3/4} (1 - x_s)^{1/4} \cos^{3/4} \phi} \right) \times \left( \psi f \frac{A_0}{A_c} \right) \left( \frac{P^{3/4}}{\omega_1^{1/4} C_d^{1/2}} \right) \quad (3)$$

The coefficient of friction ( $f$ ) is calculated by the following procedure analysed by Li and Seireg [8] and given briefly in this paper as in the thermal regime, where the sliding/rolling ratio  $> 0.27$ , the coefficient of friction can be presented as:

$$f = f_0 - [a(1 - e^b)] \quad (4)$$

with,

$$a = 0.0864 - 1.372 \times 10^3 (S_{ec}/R_c)_e \quad \text{and}$$

$$b = -(h/R_c)/(2.873(S_{ec}/R_c)_e - 2.143 \times 10^{-5})$$

where

$f_0$  coefficient of friction at  $h=0$   
 $S_{ec}$  the effective surface roughness;  $(S_{ec}/R_c)_e$ , the effective roughness parameter.

The ratio  $h_0/R_c$  in Eq. (6) represents the influence of the lubricant film. The ratio  $(S_{ec}/R_c)_e$  represents the influence of the surface condition resulting from a particular manufacturing process. The values of  $f_0$ ,  $(S_{ec}/R_c)_e$  can be found in Ref. [6] and  $h$  calculated as given by Dowson and Higginson [9].

The real contact between gear surfaces occurs at discrete areas defined by the locations where there is interaction between the surface asperities. These areas determine the primary heat generation and heat transfer surface in frictional heating.

The Greenwood–Williamson surface model [10] is used to calculate the real area of contact according to the following equation

$$\frac{A_c}{A_0} = \pi D_{sum} R_q \sigma_s F_1 \left( \frac{d}{\sigma_s} \right) \quad (5)$$

where

$\sigma_s$  the standard deviation of the summit heights  
 $D_{sum}$  the number of summits per unit area  
 $d$  the asperity height above the summit mean,  $F_1(d/\sigma_s) = \int_0^\infty (d/\sigma_s) (S - d/\sigma_s) \Phi(S) dS$  integral of the contact distribution function.

### 2.2. Temperature rise calculation based on viscous heating

Temperature rise due to viscous heating is analysed using the procedure developed by Rashid and Seireg, [11]. The model given in Fig. 2 is utilized to find the dimensionless temperature rise equations.

The model represents two rolling/sliding cylinders having different radii, thermal properties and bulk

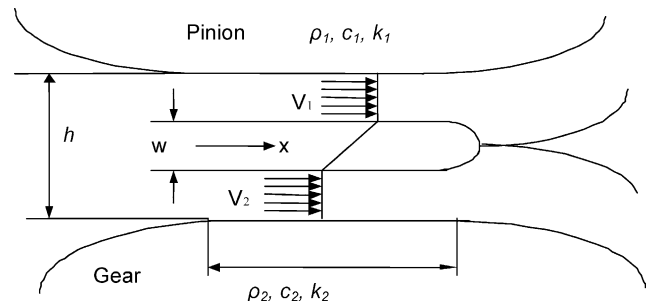


Fig. 2. Lubricated, heavily loaded sliding/rolling contact.

temperatures, which are separated by a lubricant film with thickness  $h$ . The heat generation zone with thickness  $w$  represents the liquid region where the lubricant undergoes a high shear rate. At moderate to high sliding speeds, the magnitude of  $w$  is assumed to be approximately  $0.1h$ . In order to simplify the derivation of the dimensionless equations for this case,  $w$  is initially assumed to be equal to zero. Then the equations are given as [11]:

$$\frac{T_{01} - T_{s1}}{\psi q} = \frac{1.14}{k_0} \left( \frac{V_1 \rho_1 c_1 h}{2k_0} \right)^{-0.013} \left( \frac{2b}{h} \right)^{-1.003} \times \left( \frac{k_1}{k_0} \right)^{0.013} \exp \left( -900 \times 10^{-6} \left( \frac{V_1 \rho_0 c_0 h}{2k_0} \right) \right) \quad (6)$$

and

$$\frac{T_{s1} - T_{B1}}{\psi q} = \frac{1.03}{k_1} \left( \frac{\rho_1 c_1 V_1 b}{k_1} \right)^{-0.5} \quad (7)$$

with the transient heat input  $q = V_s b \tau$  where  $\tau$  is the shear stress as  $\tau = \mu (V_s / h)$ .

### 3. The thermal and mechanical stresses

The thermal stresses for fatigue attributed to the maximum instantaneous temperature rise are calculated by using the equations given in [6] as:

$$\sigma_t = \frac{E_1 \alpha_t \Delta T}{3(1 - \nu_p)} \quad (8)$$

The maximum Hertzian contact stress ( $\sigma_m$ ) on gear tooth surface and the contact width ( $b$ ) are given below with the assumption that Poisson's ratio is 0.3 [6].

$$\sigma_m = 0.591 \sqrt{\frac{PE_{eq}}{\omega_1 r_1 R_{eq}}} \quad (9)$$

$$b = \sqrt{\frac{16}{\pi} \frac{P}{\omega_1 r_1} R_c \left( \frac{1 - \nu_1^2}{E_1} + \frac{1 - \nu_2^2}{E_2} \right)}$$

where,  $R_{eq}$  and  $E_{eq}$  are the equivalent radii of curvature and equivalent elasticity of modules, respectively.

### 4. Modification of mechanical stress combined with thermal stress

Experimental studies for investigating the repeated thermal shock stress effects on bending fatigue of two types of high-carbon (AISI 4340–4350) and low-carbon (AISI 1020) steels are reported in [6]. The tests were applied to the identical specimens with and without thermal shock

application. The results proved that the endurance limits of specimens were decreased with thermal shock applications.

The above study shows the material life is dependent on the combined mechanical and thermal stresses when the component is under application of both loads. Therefore, the following design criterion is applied in this paper.

$$1 = \sqrt{\left( \frac{\sigma_m}{K_m \sigma_u} \right)^2 + \left( \frac{\sigma_t}{K_t \sigma_u} \right)^2} \quad (10)$$

$K_m$  and  $K_t$ —calculated for high-carbon AISI 4340 steels and AISI 1020 low carbon steel by using the experimental data from experimental data given in Ref. [6] and Eq. (10). The values are given in Table 1.

A modification parameter, which shows the influence of thermal stress, is proposed. Eq. (10) can be rewritten in the form of stress ratios as below:

$$\frac{1}{\sqrt{1 + K}} = \left( \frac{\sigma_m}{K_m \sigma_u} \right) \quad (11)$$

where  $K = (K_m \sigma_t / (K_t \sigma_m))^2$  is the stress modification factor, which can be expanded by combining Eqs. (3), (8) and (9) and grouping the result as geometric, lubrication, material and surface and application factors as given by Eq. (12).  $(\sigma_m)_{all}$ ,  $(\sigma_c)_{all}$  and  $(\sigma_t)_{all}$  are the allowable mechanical, combined and thermal stresses for infinite life and experimentally found for materials given in Table 1 [6].

$$K = \left[ \frac{(1 - x_s)^{1/2} (1 + M_g)^{1/2} [1 - (M_g + 1)x_s]^2}{M_g^2 x_s^{1/2}} \times \left( \frac{\sin^{3/4} \phi}{2.36 \cos^{1/4} \phi} \right)^2 \right] \left[ \psi_f \frac{A_o}{A_c} \right]^2 \times \left[ \left( \frac{K_m}{K_t} \right)^2 E_1^2 \alpha_t^2 l \left( (1 - \nu_1)^2 \times E_c \left( \frac{1 - \nu_1^2}{E_1} + \frac{1 - \nu_2^2}{E_2} \right)^{1/2} \rho_1 k_1 c_1 \right) \right] [P^{1/2} \omega_1^{1/2} C_d] \quad (12)$$

Table 1

Factors  $K_t$ ,  $K_m$  for combined mechanical and thermal fatigue for AISI 4340 high carbon steel and AISI 1020 low carbon steel and number of cycle above endurance limit

	AISI 1020	AISI 4340
Number of cycle	$10^7$	$10^7$
$(\sigma_m)_{all}$ (N/M <sup>2</sup> )	4343	6895
$(\sigma_c)_{all}$ (N/M <sup>2</sup> )	3723	5722
$(\sigma_t)_{all}$ (N/M <sup>2</sup> )	5309	5088
$K_m = (\sigma_m)_{all} / \sigma_u$	0.63	0.53
$K_t = (\sigma_t)_{all} / \sigma_u$	0.77	0.4

Table 2  
Lubricating oil and material thermal and mechanical properties

Properties	AISI 4340 and AISI 1020	SAE 30
$E_1$ (Gpa)	205	–
$\nu_1$	0.3	–
$k$ (W/m°C)	50.2	0.13
$c$ (J/gr°C)	0.475	2.01
$\rho$ (gr/cm <sup>3</sup> )	7.85	0.88

Gear specification:  $\Phi$  (pressure angle)=20° materials physical properties (AISI 4340 and AISI 1020 steels and SAE 30 oil).

### 5. Application to gears

In this application, the allowable mechanical and thermal stresses for infinite life of the materials have been taken from the experimental study given by Seireg [6] for AISI 4340 and 1020 steels. These stresses and the temperature rise calculations presented by Taylor and Seireg [7] for the asperity contacts and Rashid and Seireg [11] for the lubricated contacts were modified for involute gear tooth profile. Results of this modification are given in this paper as a prediction and to show the importance of the thermal stresses on the gear tooth. Further experimental study, however, has to be conducted specifically on gear tooth for revision.

The applications in this study are undertaken using two extreme conditions for the viscosity. In the first, the viscosity is assumed to be constant at the inlet temperature and in the second, the viscosity is assumed to be constant at the maximum surface temperature. Two different surface manufacturing processes, fine and the rough ground, are also considered. The properties of lubricant (SAE 30) and

the materials used are given in Table 2 and all calculations are done for the 180 rad/s angular velocity of pinion.

#### 5.1. Numerical results on temperature rise

Case 1. Temperature rise is calculated at the surface and asperities for fine and rough ground gears with the assumption of constant oil viscosity corresponding to an inlet temperature (26.7 °C).

Case 2. Temperature rise is calculated for fine ground gears with the assumption of constant oil viscosity corresponding to the maximum bulk surface temperature. The viscosity temperature relationship used is given by the following Eq. (6) and found by iteration between surface temperature and viscosity. The plots of results are shown in Fig. 3.

$$\mu(T) = \mu_0 e^{755/(T_{s1}+70)} \tag{13}$$

$\mu_0$  is lubricant reference viscosity ( $\mu_0=0.97$  gr/cm s);  $T_{s1}$  is tooth surface temperature (°C).

The results show that the temperature rise increases with the decrease of the number of teeth and the increase of the gear ratio. All the temperature calculations resulting from viscous shear input are based on the two extreme assumptions of oil film viscosity either at the inlet temperature or at the maximum surface temperature. Some of the temperature rise values calculated based on these assumptions are extremely high and should be considered only as representation of trends. More realistic calculations of shear heating have to involve the change in the viscosity and other oil properties

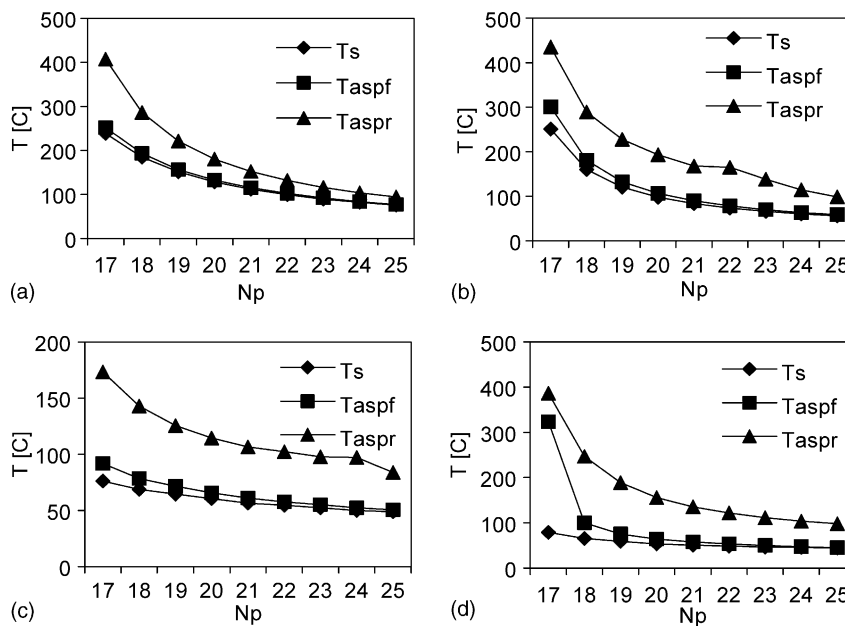


Fig. 3. Surface temperature ( $T_s$ ), asperity temperature of rough grounded surface ( $T_{aspr}$ ) and asperity temperature of fine-grounded surface ( $T_{aspf}$ ) at the start of contact of gear teeth versus number of teeth ( $N_p$ ). (a) Viscosity ( $\mu$ ) constant at inlet temperature gear ratio  $M_g=2$ , center distance  $C_d=0.254$  m. (b)  $\mu$  constant at inlet temperature  $M_g=5$ ,  $C_d=0.254$  m. (c)  $\mu$  constant at maximum surface temperature  $M_g=2$ ,  $C_d=0.254$  m. (d)  $\mu$  constant at maximum surface temperature  $M_g=5$ ,  $C_d=0.254$  m.

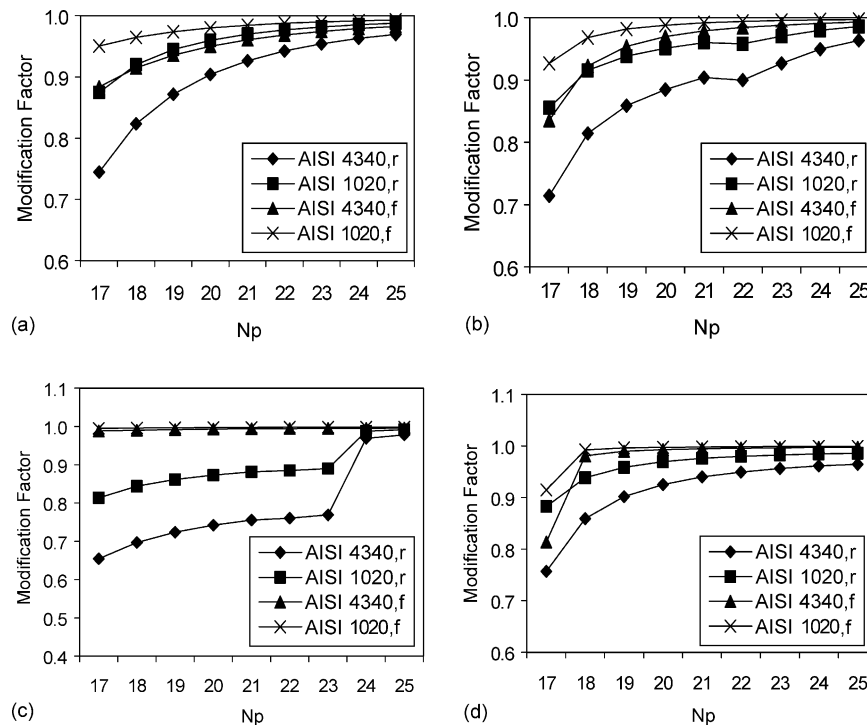


Fig. 4. Modification factor versus number of teeth ( $N_p$ ) for AISI 4340 high carbon and AISI 1020 low carbon steels with rough (r) and fine (f) grounded surface finishes. (a) Viscosity ( $\mu$ ) constant at inlet temperature gear ration  $M_g=2$ , center distance  $C_d=0.254$  m. (b)  $\mu$  constant at inlet temperature  $M_g=5$ ,  $C_d=0.254$  m. (c)  $\mu$  constant at maximum surface temperature  $M_g=2$ ,  $C_d=0.254$  m. (d)  $\mu$  constant at maximum surface temperature  $M_g=5$ ,  $C_d=0.254$  m.

gradually with temperature and pressure within film contact zone. This consideration proves computationally expensive.

From this investigation, it can be assumed that the temperature rises on the surface and on the asperities are somewhere between the calculated temperatures based on the assumed extreme conditions.

The temperature rise based on viscous shear heat input is assumed to be independent of the load applied. Further calculations are done specifically for the temperature rise on the asperities for fine and rough ground gears subjected to power of 7500 W and gear ratios of 2 and 5, respectively. The results of the calculations are given in Fig. 3. The results show that the temperature rise is highly affected by the increase of gear ratio and decrease of number of teeth. The surface roughness also affects the temperature rise indirectly. Fine ground gears are generally subjected to viscous heat input, which reduces the temperature rise at the asperities. Rough ground gears are generally subjected to frictional heat input due to the higher asperity height. Accordingly, the asperity temperature of the rough ground surface is generally higher than the fine ground surface although the bulk surface temperatures are same.

### 5.2. Numerical results on contact stress modification factor in lubricated rolling/sliding contacts

The modification factors are calculated by using the Eq. (12) for high carbon steel (AISI 4340) and low

carbon steel (AISI 1020) gears with rough and fine ground surfaces. In the case of the temperature rise calculations; the viscosity of the oil film is based on both the inlet temperature and the maximum surface temperature assumptions.

The modification parameter (Eq. (11)), which represents the mechanical component of the total allowable stress for a given number of cycles under the combined thermal and mechanical loading is also calculated and the results are plotted in Fig. 4.

The results show that high carbon steel gears are significantly more affected by the thermal stress than low carbon steel gears as a result of the higher ratio of thermal fatigue limit due to the thermal loading. Decreasing the number of teeth increases the effect of thermal stress. Fine ground gears are less influenced by thermal stress than rough ground gears.

## 6. Conclusions and recommendations

The following can be concluded from this study:

- The surface temperature rise is significantly increased for low number of pinion teeth and high gear ratios as a result of a high sliding to rolling ratio.
- Decrease on the number of teeth also decreases the allowable mechanical stress.

- The surface roughness has a significant effect on the temperature rise. Fine ground gears are generally subjected to viscous heating, which reduces the temperature rise at asperities. On the other hand rough ground surfaces are subjected to frictional heating due to the higher asperity height in relation to the oil film thickness.
- High carbon steel gears are significantly more sensitive to the thermal stress than low carbon steel as a result of lower ratio of allowable thermal strength to its ultimate strength.

The following are some recommendations for future studies on this subject:

- More accurate treatment of the effect of temperature distribution in the contact zone, on the viscosity of the lubricating film and the heat generation within the film needs to be considered.
- Investigation of the effect of the thermal conditions on the physical and chemical changes which take place in the contact zone.
- Investigation of the effect of the chemical layers that may be generated on surface as well as surface coating with different thermal properties on the surface temperature.
- Planning controlled experiments to verify the general findings of this investigation and to point to any

significant parameters that may have not been given adequate consideration in the reported study.

## References

- [1] Webster MN, Norbart CJJ. An experimental investigation of micropitting using a roller disk machine. *Tribol Trans* 1995;38(4): 883–93.
- [2] Tallian TE. Influence of asperity statistics on surface distress and spalling life of hertzian contacts. *Tribol Trans* 1993;36(1):35–42.
- [3] Lin JF, Cheng MJ, Jang JY. Tribological behaviour of steel rollers under rolling-sliding contacts. *Wear* 1991;146:149–64.
- [4] Kopf IA. Determining the loads causing progressive wear (seizing) on gear transmissions. *Soviet Eng Res* 1985;5(10):34–7.
- [5] Terauchi Y. Scoring of spur gear teeth. *Lubr Eng*. 1984;40(1):13–20.
- [6] Seireg A. Friction and lubrication in mechanical design. NY, USA: Marcel Dekker, Inc.; 1998.
- [7] Taylor TC, Seireg A. An optimum design algorithm for gear systems incorporating surface temperature. *Trans ASME, J Mech, Transm Autom*. In *Design* 1985;107:549–55.
- [8] Li Y, Seireg A. Predicting the coefficient of friction in sliding/rolling contacts. *Trans ASME, J Tribol* 1989;111:386–90.
- [9] Dowson D, Higginson GR. *Elastohydrodynamic lubrication*. Oxford: Pergamon; 1977.
- [10] Greenwood JA, Williamson JBP. Contact of nominally flat surfaces. *Proc R Soc Lond Ser A* 1966;295:300–19.
- [11] Rashid M, Seireg A. Heat partition and transient temperature distribution in layered concentrated contacts. Part I: Theoretical method. *ASME, J Tribol* 1987;109:496.